Research Article

Comparison between Two Capillary Forces Models

Pierre Lambert, Alexandre Chau, and Alain DelchambreStphane Rgnier
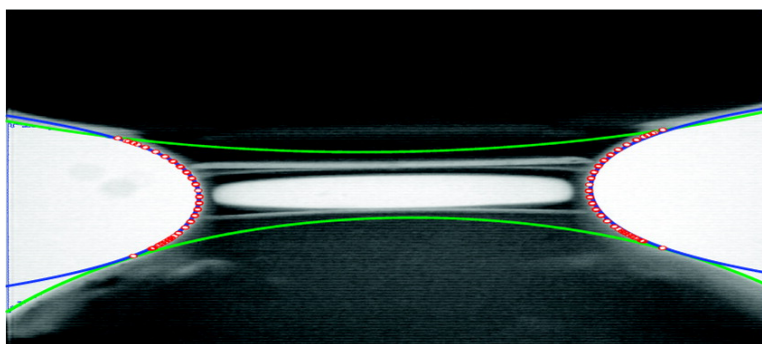
More About This Article

Additional resources and features associated with this article are available within the HTML version:

- Supporting Information
- Access to high resolution figures
- Links to articles and content related to this article
- Copyright permission to reproduce figures and/or text from this article

View the Full Text HTML

ACS Publications
High quality. High impact.

Comparison between Two Capillary Forces Models

Pierre Lambert,* Alexandre Chau, and Alain Delchambre

*BEAMS Department, Université libre de Bruxelles CP 165/14, 50 Av FD Roosevelt,
1050 Bruxelles, Belgium*

Stéphane Régnier

ISIR (ex-LRP), CNRS-Université Pierre et Marie Curie, BP61-92265 Fontenay-aux-Roses, France

Received March 26, 2007. In Final Form: December 18, 2007

Surface tension effects are dominant in miniaturization. Therefore, a lot of capillary forces models have been recently discussed in the literature. The work reported in this paper intends to prove the equivalence between two methods which are very widespread in capillary forces computation at equilibrium: the energetic method based on the derivation of the total interfacial energy and a second method summing both pressure and tension terms obtained from the meniscus profile (based on the Laplace equation). The results are supported by different qualitative arguments, an analytical proof in the case of a prism−plate configuration, numerical simulation, and experiments in the case of two millimetric spheres.

1. Introduction

With the current trend toward device miniaturization, a lot of mechanical functions are being achieved using surface tension effects which present a particularly interesting scaling behavior, since the surface tension forces linearly depend on the characteristic size. For example, let us cite the use of surface tension in micromanipulation and microassembly,[1−6] in microfluidics,[7] in optical developments,[8] and in actuation.[9] Other fields of research involve the modeling of capillary forces such as, for example, microelectromechanical system reliability and microfabrication[10−13] or capillary condensation.[14]

A lot of work has thus been reported on capillary forces modeling (see, e.g., refs 15−22) based on the so-called energetic method (i.e., derivation of the total interface energy) or on a direct force computation from the meniscus geometry, with the

latter being either determined exactly through the numerical solving of the so-called Laplace equation or approximated by a predefined geometrical profile such as a circle (i.e., toroidal approximation) or a parabola. The energetic approach is usually quite clear on its approximations: the liquid−vapor interface energy is sometimes neglected in order not to compute the exact shape of the meniscus, but an exact solution can be found if the lateral area is computed, for example, by means of a finite element solver such as Surface Evolver (see ref 23). On the contrary, literature results are not so clear as far as the other method is concerned. For example, some authors neglect the so-called tension term with respect to the Laplace term. This sometimes pertinent assumption has led many authors to add the tension term to the result obtained by deriving the interface energy, that is, to mix both methods. This paper aims at clarifying this situation by showing that the capillary force obtained by deriving the interface energy is exactly equal to the sum of the Laplace and tension terms. For this purpose, section 2 briefly reminds the principle of both methods. Their equivalence is then considered with three qualitative arguments exposed in section 3. An analytical argument is developed in section 4 in the case of the interaction between a prism and a plane. Finally, a comparison with experimental results is led in section 5, and, after a discussion in section 6, conclusions are drawn in section 7. This papers ends with an Appendix including some complements to the developments of section 4.

2. Equations

As previously explained, this paper aims at comparing two methods for capillary forces calculations, which are exposed in this section.

2.1. Laplace Approach. The so-called Laplace approach consists of determining the force from the shape of the meniscus.

$$F = F_L + F_T \tag{1}$$

where F_L is the so-called Laplace or pressure term and F_T is the so-called tensile or surface tension term. F_L arises from the pressure difference across the meniscus, which applies to the wet area of the solids in interaction. This pressure difference Δp (Pa) is described by the so-called Laplace equation, linking this

(1) Bark, K.-B. *Adhäsives Greifen von kleinen Teilen mittels niedrigviskoser Flüssigkeiten*; Springer: Berlin, 1999.
(2) Biganzoli, F. Proceedings of IEEE ISATP05, Montreal, Canada, July 19−21, 2005.
(3) Grutzeck, H. Fluidisches Greifen in der Mikrosystemtechnik. Ph.D. Thesis, TU Cottbus, 1999.
(4) Lambert, P. *Capillary Forces in Microassembly: Modeling, Simulation Experiments and Case Study*; Microtechnology and MEMS; Springer: New York, 2007.
(5) Obata, K. J. *J. Fluid Mech.* **2004**, *498*, 113−121.
(6) Pagano, C. Proceedings of the 1st CIRP−International Seminar on Assembly Systems, Stuttgart, 2006; Westkämper, E., Ed.; Fraunhofer IRB Verlag: Stuttgart, 2006.
(7) Feng, Y. *Sens. Actuators, A* **2003**, *108*, 138−143.
(8) Berge, B. *Eur. Phys. J. E* **2000**, *3*, 159−163.
(9) Borno, R. T. *J. Micromech. Microeng.* **2006**, *16*, 2375−2383.
(10) Kondo, T. *Appl. Phys. A* **2005**, *81* (8), 1583−1586.
(11) Mastrangelo, C. H. *J. Microelectromech. Syst.* **1993**, *2* (1), 33−43.
(12) Vora, K. D. *Microsyst. Technol.* **2006**, *13*, 5−6.
(13) Wu, D. *Sens. Actuators, A* **2006**, *128*, 109−115.
(14) Chau, A. *Modell. Simul. Mater. Sci. Eng.* **2007**, *15*, 305−317.
(15) Israelachvili, J. N. *Intermolecular and Surface Forces*, 2nd ed.; Academic Press: New York, 1992.
(16) de Lazzer, A. *Langmuir* **1999**, *15* (13), 4551−4559.
(17) Lambert, P. *Langmuir* **2005**, *21*, 9537−9543.
(18) Orr, F. M. *J. Fluid Mech.* **1975**, *67*, 723−742.
(19) Stifter, T. *Phys. Rev. B* **2000**, *62* (20), 13667−13673.
(20) Rabinovich, Y. I. *Adv. Colloid Interface Sci.* **2002**, *96*, 213−230.
(21) Pepin, X. *J. Colloid Interface Sci.* **2000**, *232*, 289−297.
(22) Rabinovich, Y. I. *Langmuir* **2005**, *21*, 10992−10997.
(23) Brakke, K. *Exp. Math.* **1992**, *1* (2), 141−65.
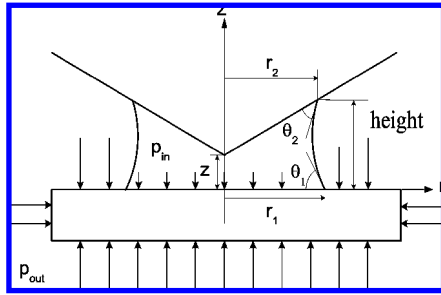
Figure 1. Axially symmetric configuration.

pressure difference to the mean curvature H (1/m) of the meniscus and the surface tension γ (N/m):

$$\Delta p = 2H\gamma \tag{2}$$

It will be noted that, according to the curvature sign of the meniscus, this Laplace term F_L can be either positive or negative. This term F_L is given by

$$F_L = \Delta p A_{SL} \tag{3}$$

where A_{SL} is the area of the solid−liquid interface of the solid on which the capillary force to compute is applied. In axially symmetric cases, A_{SL} can be replaced by (see Figure 1)

$$A_{SL} = \pi r_1^2 \tag{4}$$

where r_1 is the radius of the triple (circular) line on the solid on which the capillary force to compute is applied.

Equation 2 is valid for vanishing Bond numbers, that is, when the characteristic height of the meniscus is quite smaller than the capillary length $L_c = (\gamma/\rho g)^{1/2}$. Otherwise, the effect of the hydrostatic pressure has to be taken into account:

$$\Delta p = 2H\gamma - \rho gz \tag{5}$$

The second term F_T is due to the tensile action of the surface tension along the triple line (only the z-component, projected by $\sin \theta_1$ is here taken into account):

$$F_T = \oint \gamma \sin \theta_1 \, ds \tag{6}$$

In axially symmetric cases, F_T can be rewritten into

$$F_T = 2\pi r_1 \gamma \sin \theta_1 \tag{7}$$

An example of such a force determination in the axially symmetric case is given in ref 17.

2.2. Energetic Approach. The energetic approach is based on the derivation of the total interface energy W given by

$$W = \gamma \Sigma + \sum_{i=1}^{2} A_{SVi} \gamma_{SVi} + \sum_{i=1}^{2} A_{SLi} \gamma_{SLi} + C \tag{8}$$

where γ is the surface tension of the liquid, Σ is the liquid−vapor area, A_{SVi} (A_{SLi}) is the solid−vapor (solid−liquid) area on solid i, γ_{SVi} (γ_{SLi}) is the solid−vapor (solid−liquid) interface energy of solid i, and C is an arbitrary constant, which will be discarded by derivation at the next step. Usually, taking advantage from the link between A_{SLi} and A_{SVi}

$$A_{SLi} + A_{SVi} = C' \tag{9}$$
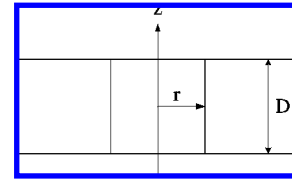
Figure 2. Case of two parallel plates separated by a gap D.

where C' is a constant and using the Young−Dupré equation, interface energies can be replaced by contact angles and surface tension:

$$\gamma_{SVi} - \gamma_{SLi} = \gamma \cos \theta_i \tag{10}$$

The total energy can now be derived with respect to the separation distance z (see Figure 1), relying on the fact that the volume of liquid is constant ($dV/dz = 0$), leading to

$$F = -\frac{dW}{dz} \tag{11}$$

Numerically, the derivative is replaced by the finite difference:

$$F = -\frac{W_{i+1} - W_i}{\Delta z_i} \tag{12}$$

An example of such force computation is described in ref 14.

2.3. Equivalence of Both Approaches. The purpose of this paper is to prove that

$$F = F_L + F_T = -\frac{dW}{dz} \tag{13}$$

3. Qualitative Arguments

The energetic approach implicitly involves both Laplace and tension terms. As a first argument, let us illustrate this in the case of two parallel plates (see Figure 2) separated by a distance D (for the need of convenience, both contact angles have been chosen equal to $\theta = \pi/2$). In this case, the total interface energy W is equal to

$$W = 2\pi rD\gamma + 2\pi r^2 \gamma_{SL} + (C' - 2\pi r^2)\gamma_{SV} + C \tag{14}$$

where γ is the surface tension of the liquid, $2\pi rD$ the lateral area of the meniscus, γ_{SL} is the surface energy of the solid−liquid interface, γ_{SV} is the surface energy of the solid−vapor interface, and C' is an arbitrary constant circular area larger than $2\pi r^2$ (it will disappear by derivation at the next step). Now, using the Young−Dupré equation ($\gamma_{SV} = \gamma \cos \theta + \gamma_{SL}$) and introducing the volume of liquid $V = \pi r^2 D$, the latter equation can be rewritten as

$$W = 2\gamma \sqrt{V\pi D} - 2\frac{V\gamma}{D} \cos \theta + \text{constant} \tag{15}$$

Since $\theta = \pi/2$, the derivation of the latter equation leads to

$$F = -\gamma \sqrt{\frac{\pi V}{D}} \tag{16}$$

which can be compared to the force established from the curvature:

$$2H = \frac{1}{r} + 0 \tag{17}$$

This leads to a pressure difference

$$\Delta p = 2H\gamma = \frac{\gamma}{r} \tag{18}$$

and henceforth to a "Laplace" term of the force equal to

$$F_L = \pi r^2 \Delta p = \gamma \sqrt{\frac{\pi V}{D}} \tag{19}$$

Note that this term is positive, that is, repulsive, because the meniscus is convex, leading to a positive pressure difference. The "tension" term of the force F_T can be written as

$$F_T = -2\pi r \gamma = -2\gamma \sqrt{\frac{V\pi}{D}} \tag{20}$$

leading to a total capillary force equal to

$$F = F_L + F_T = -\gamma \sqrt{\frac{\pi V}{D}} \tag{21}$$

Since eqs 16 and 21 are equal, we conclude that the force derived from the energy well represents both terms of the capillary force (note well that the Israelachvili approximation $F = 4\pi\gamma R \cos\theta$ proposed in eq 15.35 of ref 15 has been derived this way, consequently including both terms).

A second argument is geometric. Let us consider the case depicted in Figure 3 where both contact angles are equal to $\pi/2$: in this case, the meniscus is clearly convex, leading to a repulsive "Laplace" force which cannot be modeled by $F = 4\pi R\gamma \cos\theta$ which would lead to zero since $\theta = \pi/2$. On the contrary, if we take the (always) attractive "tension", we (qualitatively) see that we could have a total force equal to zero. This is the second argument showing that the Israelachvili approximation involves both terms, because otherwise it cannot explain the simple case of Figure 3.

A last argument is based on numerical simulation (see Figure 4). For a sphere–plane configuration and assuming $R = 13$ mm, $\gamma = 72$ mNm^{-1}, and $V = 1$ mm^3, we compared the Israelachvili approximation (solid line) with both the "Laplace" term ($\square$) and the total simulated capillary force ($\bigcirc$): we see that the Israelachvili approximation is still closer to the total force than to the "Laplace" term. Consequently, we conclude that the "tension" term is well included in this approximation.

4. Analytical Arguments

4.1. Definition of the Case Study. We propose to demonstrate the equivalence of the approaches on a 2D 1/2 prism–plane configuration. The prism is defined by its length in the y-direction (see Figure 5), L, and its angular aperture, ϕ. Its location is defined by the distance D between its apex A and the plane. Let us assume a volume of liquid V wetting the plane with a contact angle θ_1 and the prism with a contact angle θ_2. Since the curvature of the meniscus in the direction y perpendicular to the axis Ox and Oz (see Figure 5) is equal to zero, the Laplace eq 2 becomes[17]

$$\frac{x''}{(1 + x'^2)^{3/2}} = \frac{\Delta p}{\gamma} \tag{22}$$

where $x' = dx/dz$.

Assuming a vanishing Bond number, the hydrostatic pressure inside the meniscus is neglected by comparison to the Laplace pressure difference Δp, which is therefore constant in all the meniscus. Therefore, the right-hand side of eq 22 is constant, and this equation can be integrated twice with respect to z, in order to find the relation $x = x(z)$, with two integration constants
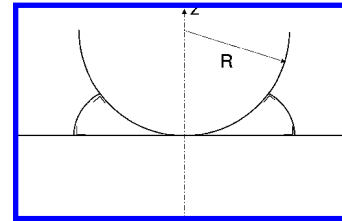
Figure 3. Sphere (radius R) and plate separated by a gap $D = 0$: contact angle $\theta = \pi/2$.
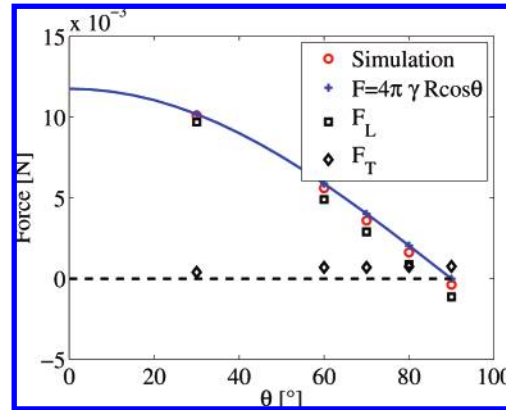
Figure 4. Case of a sphere–plate configuration with $R = 13$ mm, $\gamma = 72$ mNm^{-1}, and $V = 1$ mm^3. Comparison between the Israelachvili approximation ($F = 4\pi\gamma R \cos\theta$, solid line), the simulated "Laplace" term ($\square$), the simulated "tension" term ($\diamondsuit$), and the sum of them ($\bigcirc$). The "Laplace" and "tension" terms have been obtained using the simulation described in ref 17. Note that a positive force here denotes an attractive one.
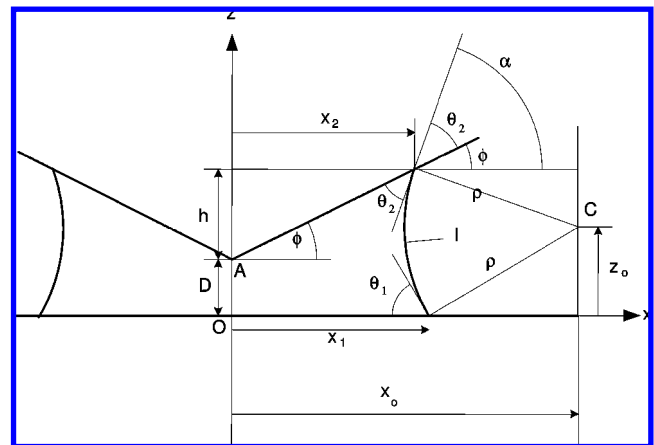
Figure 5. Prism–plane configuration.

and the undefined pressure difference Δp. A more straightforward derivation is based on the fact that since one of the curvature radii is infinite and that the total curvature $2H$ is constant, the second curvature radius $((1 + x'^2)^{3/2})/x''$ is constant: let us denote it as ρ. Therefore, the meniscus profile is a curve with constant curvature, that is, a circle given by the following equation:

$$(x - x_0)^2 + (z - z_0)^2 = \rho^2 \tag{23}$$

where x_0 and z_0 are the coordinates of the circle center. Once again, three parameters are to be determined: x_0, z_0, and ρ. This can be done using three boundary conditions: both contact angles θ_1 and θ_2 and the volume of liquid V.

4.2. Preliminary Computations. Let us express x_0, z_0, and ρ as functions of known data (ϕ, D, θ_1, θ_2) and the immersion height h, which is still unknown at this step but which will be
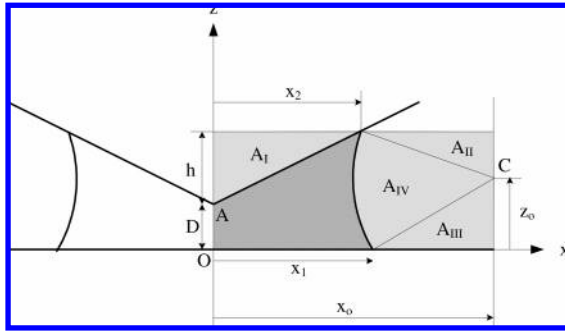
Figure 6. Determination of the immersion height from the volume of liquid.

determined using the condition on the volume of liquid V. Note that x_2 is an intermediary variable and that x_1 will be used later. For the sake of convenience, the notation $\alpha = \theta_2 + \phi$ has been adopted in the following equations:

$$x_2 = \frac{h}{\tan \phi} \tag{24}$$

$$\rho = \frac{D + h}{\cos \theta_1 + \cos \alpha} \tag{25}$$

$$z_0 = \rho \cos \theta_1 \tag{26}$$

$$x_0 = x_2 - (z_0 - D - h) \tan \alpha \tag{27}$$

$$x_1 = x_0 - z_0 \tan \theta_1 \tag{28}$$

Additional useful relations are the meniscus equation

$$x = x_0 - \sqrt{\rho^2 - (z - z_0)^2} \tag{29}$$

the meniscus slope x'

$$x' = -\frac{z - z_0}{x - x_0} \tag{30}$$

and finally, the rewritten Laplace equation linking Δp and ρ

$$\Delta p = \frac{\gamma}{\rho} \tag{31}$$

h is still to be determined using the volume of liquid V (see next step).

4.3. Determination of the Immersion Height h. The volume of liquid can be used to determine the value of the immersion height h, starting from the volume of liquid V as illustrated in Figure 6

$$V = 2LA \tag{32}$$

$$= 2L[x_0(h + D) - A_{\mathrm{I}} - A_{\mathrm{II}} - A_{\mathrm{III}} - A_{\mathrm{IV}}] \tag{33}$$

where

$$A_{\mathrm{I}} = \frac{x_2 h}{2} \tag{34}$$

$$A_{\mathrm{II}} = \frac{(x_0 - x_2)(D + h - z_0)}{2} \tag{35}$$

$$A_{\mathrm{III}} = \frac{z_0(x_0 - x_1)}{2} \tag{36}$$

$$A_{\mathrm{IV}} = \frac{\rho^2(\pi - \alpha - \theta_1)}{2} \tag{37}$$

Therefore, the equation giving the volume V can be rewritten as follows:

$$V = 2L\left[x_0(D + h) - \frac{x_2 h}{2} - \frac{\rho^2(\pi - \alpha - \theta_1)}{2} - \frac{(x_0 - x_2)(D + h - z_0)}{2} - \frac{z_0(x_0 - x_1)}{2}\right] \tag{38}$$

$$= L\{2x_2 D + x_2 h + \rho^2[\sin \alpha \cos \alpha + 2\sin \alpha \cos \theta_1 - \pi + \alpha + \theta_1 - \sin \theta_1 \cos \theta_1]\} \tag{39}$$

By noting

$$[\sin \alpha \cos \alpha + 2\sin \alpha \cos \theta_1 - \pi + \alpha + \theta_1 - \sin \theta_1 \cos \theta_1] \equiv \mu(\cos \theta_1 + \cos \alpha)^2$$

V can be further rewritten into

$$V = L\left[h^2\left(\frac{1}{\tan \phi} + \mu\right) + 2hD\left(\frac{1}{\tan \phi} + \mu\right) + \mu D^2\right] \tag{40}$$

This latter equation can be rewritten as a second degree equation with respect to the unknown h:

$$h^2 + 2hD + \frac{\mu D^2 - V/L}{\mu + \dfrac{1}{\tan \phi}} = 0 \tag{41}$$

which leads to

$$h = -D \pm \sqrt{D^2 - \frac{D^2\mu - V/L}{\mu + \dfrac{1}{\tan \phi}}} \tag{42}$$

The "−" solution makes no physical sense, since the immersion height cannot be negative. Consequently

$$h = -D + \sqrt{D^2 - \frac{D^2\mu - V/L}{\mu + \dfrac{1}{\tan \phi}}} \tag{43}$$

and the variation of h with respect to a variation of the separation distance D (it will be used in what follows) is given by

$$\frac{\mathrm{d}h}{\mathrm{d}D} = -1 + \frac{D}{D + h}\frac{1}{1 + \mu \tan \phi} \tag{44}$$

4.4. Laplace Equation Based Formulation of the Capillary Force. As it has previously been explained, the capillary force can be written as the sum of a term depending on the Laplace pressure difference Δp and the so-called tension term:

$$F = 2Lx_1\Delta p + 2L\gamma \sin \phi_1 \tag{45}$$

$$= 2L\gamma\left(\frac{x_1}{\rho} + \sin \theta_1\right) \tag{46}$$

$$= 2L\gamma\frac{x_0}{\rho} \tag{47}$$

$$= 2L\gamma\left(\frac{x_2}{\rho} + \frac{D + h - z_0}{\rho} \tan \alpha\right) \tag{48}$$

$$= 2L\gamma\left(\frac{h}{D + h}\frac{\cos \theta_1 + \cos \alpha}{\tan \phi} + \sin \alpha\right) \tag{49}$$

Using eq 43, the force can be expressed as a function of the volume of liquid V, the separation distance D, and the angles of the problem: contact angles θ_1 and θ_2 at the one hand and the prism angle ϕ at the other hand. Let us recall that $\alpha = \theta_2 + \phi$.

4.5. Energetic Formulation of the Capillary Force. As explained in section 2.2, the energetic or thermodynamic approach is based on the differentiation of the total surface energy W with respect to the separation distance D.

$$W = \gamma(\Sigma - A_1 \cos \theta_1 - A_2 \cos \theta_2) + C \tag{50}$$

where

$$\Sigma = 2Ll = 2L\rho(\pi - \alpha - \theta_1) \tag{51}$$

$$A_1 = 2Lx_1 \tag{52}$$

$$A_2 = 2L\frac{h}{\sin \phi} \tag{53}$$

Consequently, the reduced surface energy $W/(2L\gamma)$ can be written as

$$\frac{W}{2L\gamma} = \rho(\pi - \alpha - \theta_1) -$$
$$\cos \theta_1\left(\frac{h}{\tan \phi} + \rho \sin \alpha - \rho \sin \theta_1\right) - h\frac{\cos \theta_2}{\sin \phi} \tag{54}$$

Observing that the expression $(h/\tan \phi) + \rho \sin \alpha - \rho \sin \theta_1$ is equal to x_1 already defined, the reduced energy can be rewritten into

$$\frac{W}{2L\gamma} = (D + h) \times$$
$$\frac{\pi - \alpha - \theta_1 - \sin \alpha \cos \theta_1 + \sin \theta_1 \cos \theta_1}{\cos \theta_1 + \cos \alpha} -$$
$$h\left(\frac{\cos \theta_1}{\tan \phi} + \frac{\cos \theta_2}{\sin \phi}\right) \tag{55}$$

Defining $\beta \equiv (\pi - \alpha - \theta_1 - \sin \alpha \cos \theta_1 + \sin \theta_1 \cos \theta_1)/(\cos \theta_1 + \cos \alpha)$, we can further write

$$\frac{W}{2L\gamma} = D\beta + h\left(\beta - \frac{\cos\theta_1}{\tan \phi} - \frac{\cos \theta_2}{\sin \phi}\right) \tag{56}$$

To compute the force from the energy, the latter equation has to be derived with respect to D using eq 44 (β is constant with respect to D):

$$\frac{dW}{dD}\frac{1}{2L\gamma} =$$
$$\beta + \left(-1 + \frac{D}{D + h}\frac{1}{1 + \mu \tan \phi}\right)\left(\beta - \frac{\cos \theta_1}{\tan \phi} - \frac{\cos \theta_2}{\sin \phi}\right) \tag{57}$$

$$= \frac{\cos\theta_1}{\tan \phi} + \frac{\cos \theta_2}{\sin \phi} + \frac{D}{D + h}\frac{1}{1 + \mu \tan \phi} \times$$
$$\left(\beta - \frac{\cos \theta_1}{\tan \phi} - \frac{\cos \theta_2}{\sin \phi}\right) \tag{58}$$

where μ, h, and β have been defined in eqs 39, 43, and 55, respectively. All the other parameters are given data. It should be now proved that eqs 49 and 58 are equivalent.

4.6. Equivalence of Both Formulations. Equation 58 can be rewritten as

$$\frac{dW}{2L\gamma\,dD} = \frac{\cos\theta_1}{\tan \phi} + \frac{\cos\theta_2}{\sin \phi} +$$
$$\frac{D}{D + h}\left[\frac{\pi - \alpha - \theta_1 - \sin \alpha \cos\theta_1 + \sin \theta_1 \cos\theta_1}{(\cos \theta_1 + \cos \alpha)(1 + \mu \tan \phi)} - \right.$$
$$\left.\frac{1}{1 + \mu \tan \phi}\left(\frac{\cos \theta_1}{\tan \phi} + \frac{\cos \theta_2}{\sin \phi}\right)\right] \tag{59}$$

It is shown in the Appendix that the expression in brackets in eq 59 is equal to $-(\cos \theta_1 + \cos \alpha)/\tan \phi$. Therefore, eq 59 can be rewritten into

$$\frac{dW}{dD}\frac{1}{2L\gamma} = \frac{\cos \theta_1}{\tan \phi} + \frac{\cos \theta_2}{\sin \phi} - \frac{D}{D + h}(\cos \theta_1 + \cos \alpha)\frac{\cos \phi}{\sin \phi}$$
$$= [(\cos \theta_1 \cos \phi + \cos \theta_1)(D + h) -$$
$$D \cos \phi(\cos \theta_1 + \cos \theta_2 \cos \phi -$$
$$\sin \theta_2 \sin \phi)]/[(D + h)\sin \phi] \tag{60}$$

In order to let the term $\sin \alpha$ present in eq 49 to appear, let us add and subtract $\sin \alpha$ simultaneously to and from the latter equation: after some (tedious) calculations and using the relation $\alpha = \theta_2 + \phi$, the following expression can be obtained:

$$\frac{dW}{dD}\frac{1}{2L\gamma} =$$
$$\frac{h \cos \phi(\cos \theta_1 + \cos \theta_2 \cos \phi - \sin \theta_2 \sin \phi)}{(D + h) \sin \phi} + \sin \alpha$$
$$= \frac{h}{D + h}\frac{\cos \theta_1 + \cos \alpha}{\tan \phi} + \sin \alpha \tag{61}$$

As a conclusion, the latter equation leads to a force given by

$$F = -\frac{dW}{dD} = -2L\gamma\left(\frac{h}{D + h}\frac{\cos \theta_1 + \cos \alpha}{\tan \phi} + \sin \alpha\right) \tag{62}$$

The negative sign in front of $2L$ indicates that the force is attractive. Consequently, it is concluded that the force computation based on the Laplace equation (eq 49) and the result obtained from the energy formulation (eq 62) are equal.

5. Experimental Comparison Between Two Spheres

5.1. Benchmark Models. The measures which will presented in the next subsection have been compared to benchmark models, describing the capillary forces between two spheres:

(1) Reference 4 has proposed an analytical model based on the energetic method in which the lateral area of the meniscus is approximated with a cylinder for the computation of the volume

of liquid and for the contribution of the liquid−vapor interface energy to the total interface energy. As usual, the immersion height is assumed to be small. At contact ($D = 0$), the proposed model is (eq A.23 of ref 4)

$$F = -4\pi R\gamma \cos \theta \qquad (63)$$

where $1/R = 1/R_1 + 1/R_2$ and $2\cos \theta = \cos \theta_1 + \cos \theta_2$. Let us note that this equation is formally equal to the Israelachvili approximation, in which R is the radius of the sphere interacting with a plane.

(2) Reference 22 has taken a step further, giving an analytical approximation of the (assumed to be small) immersion height (eq 20 of ref 22)

$$h = \frac{D}{2}\left(-1 + \sqrt{1 + \frac{2V}{\pi R D^2}}\right) \qquad (64)$$

which can be used to compute the force at separation distance different from zero (eq 18 of ref 22):

$$F = -\frac{4\pi R\gamma \cos \theta}{1 + D/(2h)} \qquad (65)$$

These authors claim that "when the attraction force due to the vertical component of the liquid bridge is taken into account, the complete formula for the capillary force can be expressed as" (eq 19 of ref 22)

$$F = -\frac{4\pi R\gamma \cos \theta}{1 + D/(2h)} - 4\pi R\gamma \sin \alpha \sin(\theta + \alpha) \qquad (66)$$

where α is the so-called filling angle given by $\cos \alpha = 1 - h/R$.

(3) Our own numerical computations based on the energetic approach whose details are presented in ref 14.

5.2. Test Bed Description. The test bed is an atomic force microscopy (AFM)-like set up at the millimeter scale (its detailed description can be found in ref 17). In the following experiments, the liquid used is Rhodia silicone oil R47V50 ($\gamma = 20.8$ mNm^{-1}), the upper sphere is a steel ball with a diameter of 7.9 mm, and the lower ball is a ruby hemisphere with a 4 mm diameter, glued on a steel cantilevered beam, whose stiffness is of the order of 1 Nm^{-1}. The liquid was dispensed with an Eppendorf manual dispensing device (0.1−2.5 mm^3). The actual volume of liquid and the contact angles were determined with a CV500 Keyence camera (see the next section).

5.3. Procedure to Extract the Contact Angles and the Volume of Liquid. To compare experiments with simulation, the parameters of the simulation, that is, the contact angles and the meniscus volume, are evaluated based on pictures of the meniscus.

First, to estimate the contact angles, profiles of the spheres and the meniscus are fitted on the picture of Figure 7b which is obtained from a black and white conversion of Figure 7a. After a contour detection applied to Figure 7b, the spheres are fitted with circles and the meniscus is fitted with a 4th degree polynomial.

Two techniques have been compared to fit the circles: the first one assumes unknown radii and unknown center positions. They are all fitted using a least-square fit. The second technique uses a calibration of the charge-coupled device (CCD) camera optical scale using a Mitutoyo ceramic slip gauge of 1 mm thickness. Only the circles centers are then fitted. For the lower sphere, both techniques match within 1%, while, for the upper sphere, a 15% error is encountered. This is due to the limited
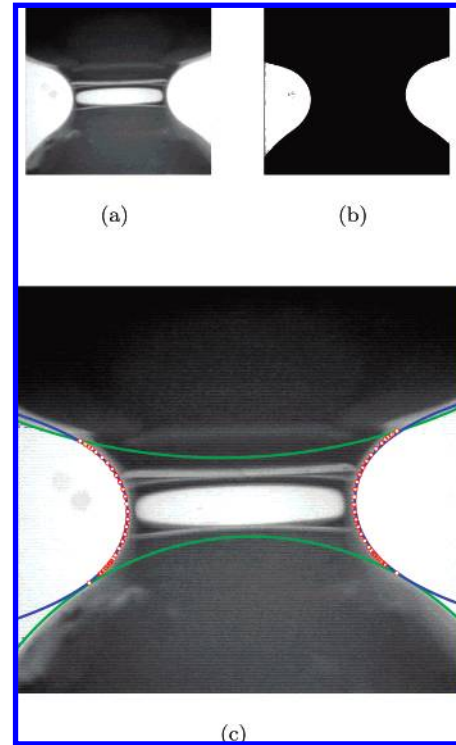
Figure 7. (a) Original picture; (b) black and white corresponding image; and (c) fitting curves: both spheres are fitted with circles (green lines), and both sides of the meniscus are fitted with a 4th degree polynomial (blue lines). Based on the contact angles given by the intersection of these fitting curves, the volume of liquid is adjusted in the simulation to fit the meniscus profile (red points).

portion of the upper sphere available for fitting. The calibration technique has thus been preferred.

Using these curves (the two circles and the two polynomials), the contact points are then computed. The contact angles are eventually evaluated using those same curves. The contact angle between the meniscus and the upper sphere is found to be in the 13−16° interval, while the contact angle between the meniscus and the lower sphere is found to be zero. One parameter that could influence the contact angle is the threshold used for contour detection. Different thresholds showed that contact angles values are kept within a ±5° interval, even for extreme values of thresholds.

Using these contact angles, computations are made with a Surface Evolver based simulation tool[14] to find a meniscus with the same neck radius as the experimental meniscus. Figure 7c shows the superposition of the actual and simulated profiles, which are in good agreement for a volume of liquid equal to $V = 1.4$ mm^3.

5.4. Measurements. During the experiments, the separation distance can be varied from contact to meniscus rupture and the corresponding force can be measured. This force is then compared with the models presented in the previous subsection.

Two volumes of liquid have been tested: $V = 0.065$ mm^3 in Figure 8 and $V = 1.4$ mm^3 in Figure 9. The values of all the parameters are given in the figure captions.

6. Discussion

Figure 8 shows a fairly good agreement between all the models. Although, eq 65 (eq 18 of ref 22) shows a better agreement with the experiments than eq 66 (eq 19 of ref 22) for small separation distances (the contrary is true for large separation distances). It is difficult to discriminate between both formulations. With the
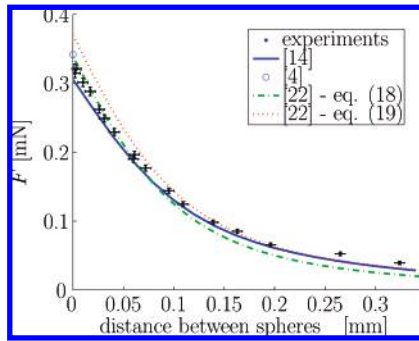
Figure 8. Capillary force as a function of the separation distance D for the following set of parameters: $R_1 = 2$ mm, $R_2 = 3.95$ mm, $\theta_1 = 0°$, $\theta_2 = 14.3°$, $\gamma = 20.8$ mNm^{-1}, and volume = 0.065 μL. The (+) symbol indicates the error crosses centered on the experimental points (●), the solid line states for the numerical simulations with $\theta_1 = 0°$ and $\theta_2 = 14.3°$, the (○) symbol states for eq 63, the dashed-dotted line states for eq 65, and the dotted line states for eq 66.
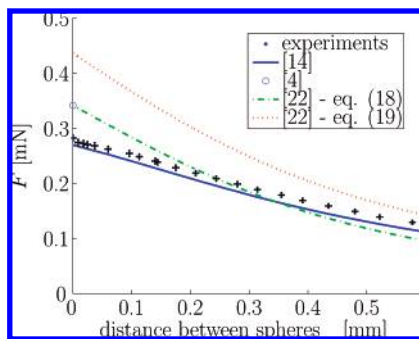
Figure 9. Capillary force as a function of the separation distance D for the following set of parameters: $R_1 = 2$ mm, $R_2 = 3.95$ mm, $\theta_1 = 0°$, $\theta_2 = 14.3°$, $\gamma = 20.8$ mNm^{-1}, volume = 1.4 μL. The (+) symbol indicates the error crosses centered on the experimental points (●), the solid line states for the numerical simulations with $\theta_1 = 0°$ and $\theta_2 = 14.3°$, the (○) symbol states for eq 63, the dashed-dotted line states for eq 65, and the dotted line states for eq 66.

volume tending to zero, the force with our numerical model tends to the analytical computations, made with the assumption of vanishing filling angles. At contact, eq 63 is quite good (it is exactly equal to eq 65 anyway).

Figure 9 shows the limitations of the approximations made with the analytical models in the case of a large volume of liquid. The analytical models do not correctly take into account the influence of the volume. The experiments and the numerical model show that, for the same experimental conditions, the volume has an influence on the force between objects. For larger volumes, the force is smaller at small distances, while it decreases slower than that for small volumes, so that the force is larger at large distances. Anyway, we see that, for large volumes, the additional tension term in eq 66 is not correct.

7. Conclusions

The contributions of this paper are twofold. First, it has been shown with three qualitative arguments and analytical developments in the case of a prism−plane interaction that two widespread capillary forces models at equilibrium are equivalent to one another: the energetic approach and the Laplace equation based approach. Second, it has been shown how powerful the analytical approximations of eqs 63 and 65 are in the case of small volumes of liquid. In this case, both formulations (eqs 65 and 66) are more or less in the uncertainty domain, so that one cannot be said to be more exact than the other (the first one seems to be better

at small separation distances and conversely). In the case of larger volumes of liquid, it has been shown that no analytical approximation could predict the experiments very accurately (however, they give an excellent order of magnitude). In the case of our experiments, it seems that the additional term introduced in eq 66 would not be necessary, leading to a less accurate prediction. The numerical simulation is in fairly good agreement with experiments in all cases. Therefore, this numerical tool will be used in the future to compute the validation limits of all the analytical approximations, according to a given uncertainty interval. An inherent limitation of all the discussed models, analytical or numerical, is that they rely on equilibrium assumptions. Therefore, a perspective is to investigate the dynamics of these forces.

Appendix

$$\frac{dW}{2L\gamma\,dD} = \frac{\cos\theta_1}{\tan\phi} + \frac{\cos\theta_2}{\sin\phi} + \frac{D}{D+h} \times$$
$$\left[\frac{\pi - \alpha - \theta_1 - \sin\alpha\cos\theta_1 + \sin\theta_1\cos\theta_1}{(\cos\theta_1 + \cos\alpha)(1 + \mu\tan\phi)} - \right.$$
$$\left.\frac{1}{1 + \mu\tan\phi}\left(\frac{\cos\theta_1}{\tan\phi} + \frac{\cos\theta_2}{\sin\phi}\right)\right] \quad (67)$$

In this latter equation, let us replace the expression in brackets by a new parameter B, which can be reduced to a common denominator. Using eq 39 to replace μ and $\alpha = \theta_2 + \phi$, we then find

$$B = -\frac{\cos\phi(\cos\theta_1 + \cos\alpha)}{\sin\phi} \quad (68)$$

and the surface energy derivative given by eq 59 can be rewritten into

$$\frac{dW}{2L\gamma\,dD} =$$
$$\frac{\cos\theta_1}{\tan\phi} + \frac{\cos\theta_2}{\sin\phi} - \frac{D}{D+h}\frac{\cos\phi(\cos\theta_1 + \cos\alpha)}{\sin\phi} \quad (69)$$

Adding and subtracting $\sin\alpha$, the latter equation can be written as follows:

$$\frac{dW}{2L\gamma\,dD} = \frac{\cos\theta_1}{\tan\phi} + \frac{\cos\theta_2}{\sin\phi} - \frac{D}{D+h} \times$$
$$\frac{\cos\phi(\cos\theta_1 + \cos\alpha)}{\sin\phi} - \sin\alpha + \sin\alpha$$
$$= \sin\alpha + \frac{h}{D+h}\frac{\cos\theta_1 + \cos\alpha}{\tan\phi} \quad (70)$$

The latter equation is equal to eq 49, which demonstrates the equivalence between the Laplace equation based and energetic force formulations.